INSTITUTO DE FÍSICA

preprint

IFUSP/P-154

MEASUREMENT OF THE GIANT E2 AND M1 RESONANCES FOR ^{236}U

by

J.D.T.Arruda Neto, B.L.Berman, S.B.Herdade and I.C.Nascimento

Instituto de Física, Universidade de São Paulo

UNIVERSIDADE DE SÃO PAULO
INSTITUTO DE FÍSICA
Caixa Postal - 20.516
Cidade Universitária
São Paulo - BRASIL

1758155

MEASUREMENT OF THE GIANT E2 AND M1 RESONANCES FOR ^{236}U†

J. D. T. Arruda Neto, B. L. Berman*, S. B. Herdade, and I. C. Nascimento

Instituto de Física
Universidade de São Paulo
São Paulo, Brasil

ABSTRACT

The yields and angular distributions of fission fragments from the electrofission of ^{236}U have been measured with fission-track detectors for incident electron energies from 5.5 to 26.5 MeV. Analysis of these data, combined with the known photofission cross section, results in the simultaneous determination of (a) an E2 giant resonance for this nucleus located at 10.8 ± 0.4 MeV, having a width of 8 ± 1 MeV, and exhausting 88 ± 11% of the EWSR (energy-weighted sum rule), and (b) an M1 giant resonance at 5.8 ± 0.2 MeV whose strength is about 2% of that of the E2 giant resonance.

NUCLEAR REACTIONS: ^{236}U (e, f); measured fission-fragment yields and angular distributions from 5.5 to 26.5 MeV; deduced characteristics of E2 and M1 giant resonances. PACS Numbers: 25.30, 25.85.

This paper was prepared for submittal to Physical Review Letters.

SET/78

Among the new giant resonances discovered in the last few years, the isoscalar electric quadrupole resonance (GQR) has been the primary focus of many studies[1,2]; interest in the magnetic dipole resonance (GMR) has been growing as well.[2]

We have determined the characteristics of both the GQR and the GMR for ^{236}U, using a new technique, which consists of the simultaneous analysis of nuclear electro- and photoexcitation by means of the formalism of virtual-photon theory in the distorted-wave Born approximation (DWBA). A recent study of ^{238}U using the same approach[3] also detected the GQR as well as a significant M1 component in the photofission reaction channel. The two measurements are compared below.

Nuclear electroexcitation is a powerful tool for the study of multipolar components other than the dominant electric-dipole component in photonuclear reactions, such as E2 and M1, because the virtual-photon spectra for E2 and M1 transitions are enhanced greatly (under certain conditions) over the E1 virtual-photon spectrum.[4,5] Thus, measurements which would be exceedingly difficult with real photons become relatively straightforward with virtual photons.

The experimental information needed in order to obtain the E2 and M1 components in the photofission channel are (a) the electrofission yield curve, (b) the electrofission-fragment angular distributions near the fission barrier, and (c) accurate photofission cross-section data (measured with real photons). This last information is available from recent measurements performed by a joint Los Alamos-Livermore collaboration at Lawrence Livermore Laboratory[6]; in addition, a valuable check on the final results can be made with the aid of detailed photofission-fragment angular-distribution data obtained recently by Alm and Lindgren at Lund.[7]

The electrofission yields and angular distributions reported here were obtained by irradiating thin ($\lesssim$ 200 μg/ cm^2) targets of ^{236}U with the electron beam of the University of São Paulo Linear Accelerator, in steps of 0.25 MeV from 5.5 to 12 MeV, 0.5 MeV from 12 to 15.5 MeV, and 1 MeV from 15.5 to 26.5 MeV. Bremsstrahlung-induced fission yields were measured for end-point energies of 11, 13, 15, 17, and 19 MeV in order to normalize the electrofission yields to the photofission cross section of Ref. 6. The fission fragments were detected using mica-foil track detectors. Details of the accelerator and beam characteristics, the reaction chamber, beam monitoring devices, and detection technique have been described previously.[8]

The electrofission yield Y, as a function of incident electron energy E_0, is given by

$$Y(E_0) = \sum_{\lambda L} \kappa \int_0^{E_0} \sigma^{\lambda L}(E)\, N^{\lambda L}(E,E_0)\, E^{-1}\, dE \qquad (1)$$

where λ identifies the electric or magnetic character of the transition and L its multipolarity, $N^{\lambda L}$ is the virtual-photon spectrum calculated in DWBA,[4] E is the real or virtual photon energy, κ is the normalization constant, and the photofission cross section σ is given by

$$\sigma(E) = \sum_{\lambda L} \sigma^{\lambda L}(E) \ . \qquad (2)$$

For λL limited to E1, E2, and M1, one can eliminate σ^{E1}, group terms, and apply certain small approximations[3] to obtain the yield difference

$$\Delta Y(E_0) \equiv Y(E_0) - \kappa \int_0^{E_0} \sigma(E) N^{E1}(E,E_0)\, E^{-1} dE$$

$$= \kappa \int_0^{E_0} \sigma^{Add}(E) \left[N^{E2}(E,E_0) - N^{E1}(E,E_0) \right] E^{-1} dE \qquad (3)$$

where

$$\sigma^{Add}(E) = \sigma^{E2}(E) + F(E)\sigma^{M1}(E) \qquad (4)$$

and $\langle F(E) \rangle = \left\langle \frac{N^{M1}}{N^{E2}} \right\rangle$ is 3.1 ± 0.2 near 6 MeV (Ref. 4).

The experimental results for the normalized yield Y/K are shown in Fig. 1(a), in which the solid curve represents $\int_0^{E_0} \sigma(E) N^{E1}(E,E_0) E^{-1} dE$, and the values for $\sigma(E)$ were obtained from Ref. 6. The normalized yield differences between the electrofission data and the curve in Fig. 1(a) are shown in Fig. 1(b); Fig. 1(c) shows $\sigma^{Add}(E)$ obtained by solving the integral equation (3) using the least-structure unfolding method of Cook.[9] The present analysis for ^{236}U represent an improvement over the previous ones for ^{238}U (Ref. 3) primarily because of the use of the more accurate data for $\sigma(E)$ from Ref. 6; an indication of this is the fact that the χ^2 of the unfolding process for ^{236}U is 0.97, whereas that for ^{238}U was 1.20.

The cross section $\sigma^{Add}(E)$ is the sum of the E2 part and an amplified [by $F(E)$; see Eq.(4)] M1 part which manifests itself mainly between 5.5 and 6.5 MeV; the peak in σ^{Add} at 5.8 MeV is the first evidence of the GMR. The separation and delineation of these two components is accomplished by use of the electrofission angular distributions, given by the differential cross section

$$\frac{d\sigma_e(E_0,\theta)}{d\Omega} = A(E_0) + B(E_0) \sin^2\theta + C(E_0) \sin^2 2\theta. \qquad (5)$$

The points shown in Fig. 2(a) represent the coefficient $C(E_0)$, obtained by least-squares fits of Eq. (5) to the data. Assuming that near 6 MeV all the E2 fission reactions proceed via the K=0 channel

we have[10]

$$C(E_0) = (45/64\pi) \int_0^{E_0} \sigma^{E2}(E)\left[N^{E2,1} - 3N^{E2,0} - 0.5\ N^{E2,2}\right] E^{-1} dE \qquad (6)$$

where the $N^{E2,M}$ are the E2 virtual-photon spectra for each magnetic substate M. The dashed curve in Fig. 2(a) is obtained from Eq.(6) for the case $\sigma^{E2}=\sigma^{Add}$ (no M1 component); a large discrepancy between it and the data is observed. However, assuming the existence of an M1 resonance with a Breit-Wigner shape at 5.8 MeV, 1 MeV wide, and 0.4 mb peak cross section [see Fig. 1(c)], subtracting it from σ^{Add} [taking into account the amplification factor F(E)], and again integrating Eq.(6), we obtain the solid curve in Fig. 2(a). This curve agrees with the experimental data up to $\sim$ 6.5 MeV; above this energy, the opening of additional K-channels is expected. This procedure also has been performed for the photofission angular distributions,[7] with similar results. In Fig. 2(b) the points represent the values for σ^{E2} obtained from

$$\sigma^{E2}(E) = \frac{(8/15)c(E)}{a(E) + (2/3)b(E) + (8/15)c(E)}\ \sigma(E) \qquad (7)$$

for the K=0 channel. The values for the coefficients a, b, and c are taken from the photofission data of Ref. 7, and $\sigma(E)$ again is from Ref. 6. The good agreement observed in Fig. 2(b) enables us to conclude again that the parameters of the GMR are close to those assumed above. Three points should be noted here: (a) in the absence of an M1 component, σ^{E2} is given directly by σ^{Add}; (b) even a small M1 component produces a large electron fission yield since F(E) is large in the low-energy region, thus demonstrating the great sensitivity of the virtual-photon technique to the GMR; and (c) the low-energy region (from 5 to 8 MeV) is where the greatest confidence in this method of analysis can be placed.

The parameters of the GQR and GMR for ^{236}U, together with those for ^{238}U from Ref. 3, are listed in Table I. Salient features of these results are: (a) peak energies for both the GQR ($67A^{-1/3}$) and the GMR ($36A^{-1/3}$) agree well with the experimental systematics for heavy nuclei[1,2]; (b) the width of the GQR is large compared with that for other heavy nuclei, possibly resulting from a substantial splitting[3] of the GQR for these deformed[6] nuclei; (c) the large fraction ($88 \pm 11\%$) of the E2 EWSR for ^{236}U that is exhausted shows that the GQR for this nucleus decays mostly, if not entirely, through the (γ,f) channel; and (d) the results for ^{236}U are close to those for ^{238}U, as might have been expected.

Finally, it should be stressed emphatically that the method of analysis employed in this work requires a precise knowledge of both electro- and photoexcitation data (as well as of the virtual-photon spectra) in order to determine unambiguously the role played by multipolar components other than E1 in the nuclear photoabsorption process. Given that precise knowledge, however, the important systematics of both the GQR and the GMR, for the actinide region of the periodic table in particular but for all other nuclei as well, can be learned.

We are pleased to acknowledge the able assistance of Alvaro Vannucci, Lucia Setiuko Tengan, and Rosana Hermann in preparing the mica foils and handling the data. We benefited as well from valuable discussions with Professor G. Moscati, Dr. E. Wolynec, Professor J. Goldemberg, and Dr. J. T. Caldwell. Finally, thanks are due to Dr. J. G. Povelites of Los Alamos Scientific Laboratory for preparing the uranium target foils.

REFERENCES

†Work supported in part by the Fundação de Amparo à Pesquisa do Estado de São Paulo and the Conselho Nacional de Pesquisas. A preliminary account of this work appeared as an abstract in Ciência e Cultura (1978).

*Permanent address: Lawrence Livermore Laboratory, University of California, Livermore, California 94550, U.S.A.

[1]G. R. Satchler, Phys. Reports 14, 97 (1974).

[2]S. S. Hanna, in Proc Int. School Electro- and Photonuclear Reactions, Erice, Italy (1976).

[3]J. D. T. Arruda Neto, S. B. Herdade, B. S. Bhandari, and I. C. Nascimento, Phys. Rev. C (in press).

[4]W. W. Gargaro and D. S. Onley, Phys. Rev. C 4, 1037 (1971).

[5]I. C. Nascimento, E. Wolynec, and D. S. Onley, Nucl. Phys. A246, 210 (1975).

[6]J. T. Caldwell, E. J. Dowdy, B. L. Berman, R. A. Alvarez, and P. Meyer, Los Alamos Scientific Laboratory Report No. LA-UR 76-1615 (1976) and to be published.

[7]A. Alm and L. J. Lindgren, Nucl. Phys. A271, 1 (1976).

[8]J. D. T. Arruda Neto, B. S. Bhandari, S. B. Herdade, and I. C. Nascimento, Phys. Rev. C 14, 1499 (1976).

[9]B. C. Cook, Nucl. Instrum. Methods 24, 256 (1963).

[10]J. D. T. Arruda Neto, S. B. Herdade, and I. C. Nascimento, "Formalism and Applications of Electro- and Photofission Fragment Angular Distributions," University of São Paulo preprint (1978).

Table I. Parameters of the GQR and GMR

Nucleus and Multipolarity	Peak Energy (MeV)	Width (MeV)	Strength (MeV-mb)	Percent of EWSR (%)
^{236}U (this work):				
E2	10.8 ± 0.4	8.0 ± 1.0	35 ± 5	88 ± 11
M1	5.8 ± 0.2	∿1.0	∿0.6	
^{238}U (Ref. 3):				
E2	9.9 ± 0.2	6.8 ± 0.4	∿30	71 ± 7
M1	6.5 ± 0.4	∿1.5	∿ 1	

FIGURE CAPTIONS

Fig. 1 (a) Normalized measured electrofission yield for ^{236}U (data points). The solid curve represents the yield which would result from the E1 component only, obtained by integrating the photofission cross-section data of Ref. 6.

(b) Normalized electrofission yield difference between the data and the curve of Fig. 1 (a) (data points). The solid curve is the fold-back of σ^{Add} in Eq. (3).

(c) Photofission cross sections obtained from the yield analysis: solid curve with error band – σ^{Add}; middle solid curve – σ^{E2}; lower solid curve – σ^{M1}.

Fig. 2 (a) Coefficient of the $\sin^2 2\theta$ term in the electrofission differential cross section obtained from the measured angular distributions for ^{236}U (data points). The solid curve represents this coefficient as computed from σ^{Add} after M1 subtraction; the dashed curve assumes no M1 component in σ^{Add}.

(b) E^2 photofission cross section obtained from the total photofission cross-section data of Ref. 6 and the angular-distribution data of Ref. 7 (data points). The solid curve with the error band is σ^{E2} from Fig. 1 (c); the upper solid curve is σ^{Add} from Fig. 1 (c) (which assumes no M1 component).

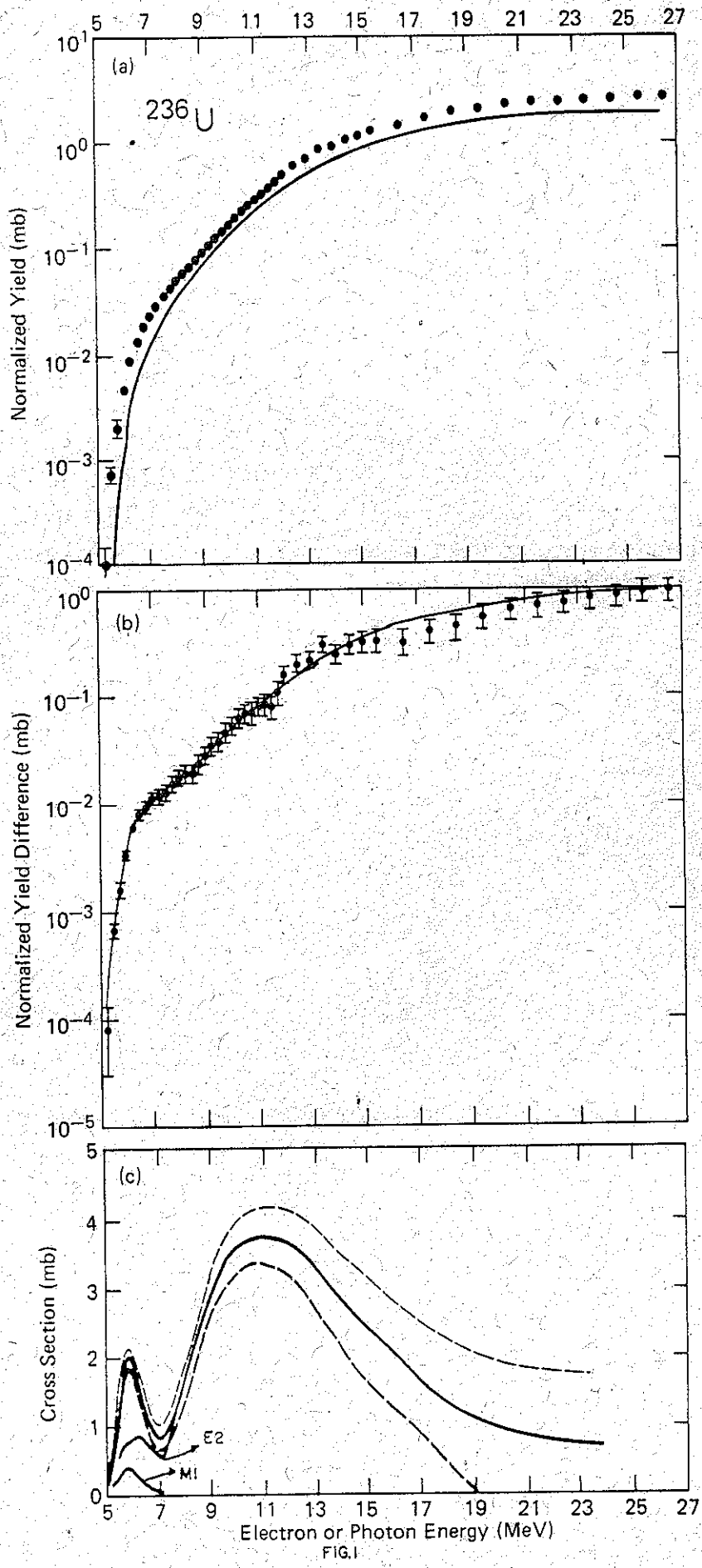
(a)
^{236}U
Normalized Yield (mb)
(b)
Normalized Yield Difference (mb)
(c)
Cross Section (mb)
E2
M1
Electron or Photon Energy (MeV)

FIG. 1

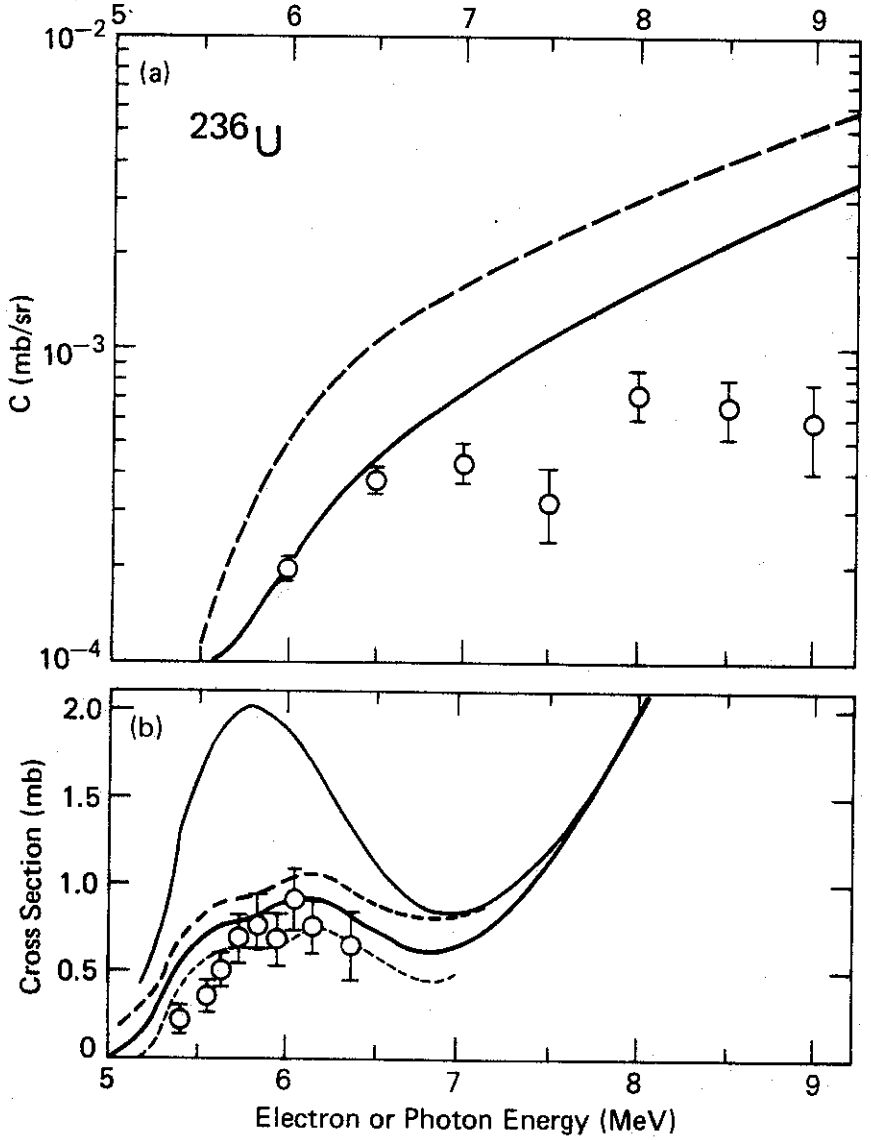
(a)
^{236}U
C (mb/sr)
10^{-2}
10^{-3}
10^{-4}
5
6
7
8
9
(b)
Cross Section (mb)
2.0
1.5
1.0
0.5
0
Electron or Photon Energy (MeV)

FIG. 2